Fermi National Accelerator Laboratory

Techniques for Measurement of Dipole Endfields with a Rigid Integrating Coil

Henry D. Glass

Fermi National Accelerator Laboratory
P.O. Box 500, Batavia, Illinois 60510

Disclaimer

Techniques for Measurement of Dipole Endfields With a Rigid Integrating Coil

Henry D. Glass

*Fermi National Accelerator Laboratory**
P.O. Box 500, Batavia, IL 60510

Abstract

The endfield is often one of the most critical regions in conventional accelerator magnets. While the magnetic field structure of dipole ends can be complicated, it can be well described by a few parameters which include the effective magnetic length, L_{eff}, and the integrated harmonics. Both of these parameters can be measured using a rigid coil which measures $\int Bdl$ in the endfield region as a function of insertion depth z and transverse displacement x. We employ a data analysis technique which uses these measurements to remove body field contributions to the end field integral, resulting in the effective integrated endfield shape. A least squares polynomial fit is then used to estimate the harmonic coefficients up to decapole. We also present the technique for measuring L_{eff} as a function of magnet current. These measurement techniques were successfully used in a study to finalize the design of the endpacks for the Fermilab Main Injector Dipole. The techniques are sufficiently general to be useful for other applications, such as the testing of the SSC Medium Energy Booster endpacks.

I. INTRODUCTION

We describe endfield measurement techniques that were developed for studying various endpack designs for magnet IDM002, the 2nd prototype dipole for the Main Injector[1]. The endpacks were measured using a 2.032 m long rigid probe called a Flatcoil. The probe has 24 turns of 0.254 mm diameter wire wound around an aluminum bar of width 0.635 cm. The turns were spaced in a geometry which minimizes the sextupole contribution of the flux, as expanded about the probe center. The total flux, summed over all turns, is very nearly proportional to the field integral along a path running down the geometrical center of the probe. The probe was mounted on a movable stand which allowed us to insert the probe to various depths inside the magnet. In the *baseline* mode of operation, the

probe records the difference in flux between zero current and current i.

By aligning the long axis of the probe with the longitudinal (z) axis of the magnet, we easily recover the integrated field over the length of the probe:

$$J(z_1, z_2) = \int_{z_1}^{z_2} B(z)dl = \frac{\Delta\Phi}{Nw},$$

where N is the number of turns and w is the probe width; z_1 ansd z_2 are the endpoint coordinates of the probe. We used a coordinate system where z is zero at the first lamination of the endpack, and is positive going into the magnet. This relation between field integral and flux does not include a correction for the remnant field.

We positioned the probe so that z_1 is far outside the magnet, in a region where the field is negligible. One may therefore approximate z_1 as being equal to $-\infty$. The integral then becomes a function solely of the endpoint of the probe that is inside the magnet.

For the endfield shape measurements, data were acquired using Flatcoil probe in the *scan* mode, in which the magnet current is kept constant and the probe scans horizontally across the magnet aperture. By positioning one end of the probe a depth z_0 inside the magnet (the other end being outside the magnet), we measured the field integral as a function of depth and transverse position.

II. EFFECTIVE LENGTH

A. Measurement Procedure

We measured the field integral at up to 10 different currents and over a range of probe depths, $0 < z < 50.8$ cm, stepping every 5.08 cm in z. At each position the data acquisition program (running on a VAX) recorded the measurements of the current, the z position, and the flux to a data file. The z position was the only quantity of the measurement process under manual control, both in terms of positioning (via alignment with a steel ruler mounted on the test stand), and recording.

B. *Effective Length Calculation*

The total effective length for a magnet excited to a specified current i is

$$\mathcal{L}_{\text{eff}}(i) = \frac{\int_{-\infty}^{\infty} B(i,z)dl}{B_0(i)} \qquad (1)$$

where B_0 is the mean body field. The total integral may be measured using a probe which extends the entire length of the magnet, and B_0 may be measured by a probe which samples only the body field. In a high quality dipole, the body field is very uniform, only falling off as one approaches close to the ends. With this observation in mind, we can re-express Eq. 1 in terms of the steel length, L_s, and a quantity L_{end} which we call the *end effective length*:

$$\mathcal{L}_{\text{eff}}(i) = L_s + 2L_{\text{end}}(i) \qquad (2)$$

The factor of 2 is present because of our definition that L_{end} is the effective length of each end of the magnet.

We used a measurement procedure which measures L_{end} using the 2.03 m probe. If the probe is inserted a distance z into the magnet, then the quantity

$$\ell(z) = \frac{J(z)}{B_0} - z \qquad (3)$$

should become constant and approach L_{end} as z becomes larger. The body field, B_0, is determined by performing a linear fit to $J(z)$. The slope is identified as the mean body field in the region $z_{min} < z < z_{max}$ over which the fit is made.

The relative effective length describes the change in L_{end} with current and can be determined by choosing a reference current, i_0, and using Eq. 3 to obtain

$$\Delta\ell(i,z) = \ell(i,z) - \ell(i_0,z) = \frac{J(i,z)}{B_0(i)} - \frac{J(i_0,z)}{B_0(i_0)} \qquad (4)$$

The average of $\Delta\ell(i,z)$ for $z > z_{min}$ is used as the value of $\Delta L_{\text{end}}(i)$. One may see from Eq. 4 that this quantity is insensitive to positioning errors in z, a dominant source of systematic errors.

Using the procedure described above we calculated $L_{\text{end}}(i)$ and $\Delta L_{\text{end}}(i)$ for each endpack. The results are presented in [2].

C. *Error estimates*

A set of measurements was taken in order to understand the contribution of z positioning errors to the total error in the flux. First, we took four runs at 1500 A with the probe fixed at $z = 50.8$ cm. These runs produced a standard deviation of the flux equal to $\sigma_\Phi/\Phi = 1.6 \times 10^{-5}$. This error was identified as being due to a combination of electronic readout noise and accuracy in magnet current readout. Another four runs were then taken, in which the probe was removed and then repositioned at $z = 50.8$ cm prior to each run. In this case we obtained $\sigma_\Phi/\Phi = 3.6 \times 10^{-4}$,

which we attribute to the combined influence of noise plus z positioning errors. The error due to z positioning alone is then estimated from these data to be 0.18 mm. Averaging the results of this procedure at selected z positions gave 0.13mm, which led to a systematic error in L_{end} of 0.37 mm.

Some endpacks were measured more than once, usually to determine measurement repeatability or to understand the effect of varying some of the measurement conditions. A test of the long-term repeatability of these measurements was done by comparing measurements of Endpack 1 taken one year apart. During this interval, not only had the endpack been removed and subsequently remounted, but the magnet itself had been removed from the test stand for a period of time. The agreement between the two data sets is very good, beng typically 0.2 mm at most currents.

III. FIELD SHAPE MEASUREMENTS

This section describes how the endfield harmonics were estimated from measurements of $J(x, z_0)$. At each selected current we measured $J(x,z)$ over the longitudinal range $0 < z < 50.8$ cm in 5.08 cm steps. At each z position we scanned transversely from $-6.35\text{cm} < x < +6.35$ cm in 0.254 cm steps. Four scans were made at each z, and for each x position we recorded the average of the four scans and the standard deviation in the data file. We inserted the probe at an angle of $0.6°$ with respect to the lamination face, which coincides with the beam direction.

A. *Body field / End field separation*

The first step in the data analysis was to separate the component of the flux that is attributable to the end field from the body field. For probe positions $z > z_{min}$, where z_{min} is the location inside the magnet beyond which end effects are unimportant, we can make a linear approximation to the field integral as a function of z:

$$J(x,z) = \alpha(x) + \beta(x)z \qquad (5)$$

The function $\beta(x)$ can be identified as the body field shape, $B(x)$. We can identify $\alpha(x)$ as the effective end field integral:

$$\alpha(x) = \int_{-\infty}^{end} B(x,z)dz \qquad (6)$$

That is, it is the field integral over some region containing the end of the magnet, with the body contribution subtracted. Note that we do not specify precisely what the upper limit on this integral is, nor do we need to, as long as the probe integrates over a region at least as large as any region in which end effects are important. This is equivalent to choosing z_{min} large enough so that $B(z_{min})$ contains only body field. For this analysis we chose $z_{min} = 25.4$ cm. The error estimated for each $J(x,z)$ was determined from the measured standard deviation in the flux and an estimate of the z positioning error.

B. *Endfield shapes*

Figure 1 shows a superimposed view of all Endpack field shapes at 1500 A. The field shapes are the endfield integrals of Eq. 6 normalized by the quantity $B_0 L$ and multiplied by 10^4. The endfield shapes are observed to be approximately independent of current. The distinct two-hump shape seen in many of the endfields can be parameterized by a large positive sextupole combined with a weaker negative decapole. The magnitude of the sextupole is correlated with the size of the noses on the endpacks. Endpack 10 is seen to have the most desirable shape, in that its deviation from zero is smaller than any of the others.
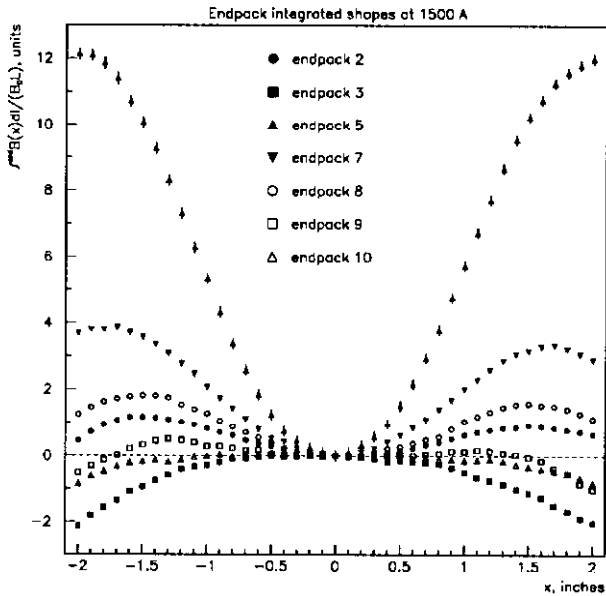

Figure 1: Integrated field shapes for all endpacks.

C. *Estimation of normal harmonics*

We obtain the normal harmonics by fitting the function $\alpha(x)$, obtained from Eq. 5 to a polynomial:

$$\alpha(x) = \sum_{n=0}^{p} J_n x^n \qquad (7)$$

Prior to performing the fit, the dipole term, $\alpha(0)$ is subtracted from $\alpha(x)$; this defines an endfield shape function, $s(x) = \alpha(x) - \alpha(0)$. In subtracting this constant from $\alpha(x)$, we also remove the systematic error due to the probe z positioning error, since this source of error is the same for all values of x. We note that there is a simple relation between the effective length due to the endfield and this dipole term[2]:

$$L_{eff} = \frac{\alpha(0)}{\beta(0)} \qquad (8)$$

The fit parameters J_n in Eq. 7 are identified as the integrated normal harmonics over the end region. We chose to report results in terms of normalized harmonics, where the normalization is relative to the body dipole integrated over the length of the magnet:

$$b_n = \frac{J_n}{B_0 L} \qquad (9)$$

The value to choose for p and the region in x over which to perform the fit were chosen experimentally. Strictly speaking, one may not perform a harmonic fit over a region larger than a circle that just fits within the magnet aperture. Inside the body of the Main Injector magnet, the vertical aperture is 5.08 cm and the horizontal aperture is wide open. Body field shapes are theoretically constrained to be fitted over regions $x_{min} < x < x_{max}$ such that $x_{max} - x_{min} < 5.08$ cm. Note that we are only considering regions that are centered vertically ($y = 0$), and therefore skew harmonics can be neglected. At the ends, however, the vertical aperture opens up as a function of z, and the formal constraints on the fit region become less severe. We chose to fit over the region $|x| < 5.08$ cm. With regard to the proper choice of p, we note that for dipoles one may expect important decapole contributions, which suggests choosing p at least as large as 4; the next "allowed" harmonic after decapole is 14-pole, corresponding to $p = 6$. We tried both 4 and 6; the fit to Endpack 10 indicates a need to use $p = 6$ to achieve a good fit at the higher currents. The results are reported in [3, 4].

IV. ACKNOWLEDGMENTS

REFERENCES

[1] Fermilab Main Injector, Title I Design Report, August, 1992.

[2] H. Glass et. al., "Effective Length Measurements of Main Injector Dipole Endpacks," Fermilab TM-1815, Dec. 1992.

[3] H. Glass et. al., "Field Shape Measurements of Main Injector Dipole Endpacks," Fermilab TM-1820, Dec. 1992.

[4] D. Harding et. al., "Design and Measurements of Prototype Main Injector Dipole Endpacks," in *Proceedings of the 1993 Particle Accelerator Conference, Washington, DC, May 17-20, 1993*. Institute of Electrical and Electronic Engineers, 1993.